Water and Methanol Adsorption on MgO(100)/Mo(100) Studied by Electron Spectroscopies and Thermal Programmed Desorption

J. Günster, G. Liu, J. Stultz, S. Krischok, and D. W. Goodman*

Department of Chemistry, Texas A&M University, College Station, Texas 77842-3012

Received: June 22, 1999; In Final Form: April 13, 2000

The adsorption of methanol (CH_3OH) and water (D_2O) on the MgO(100)/Mo(100) surface at 100 K has been studied by metastable impact electron spectroscopy (MIES), ultraviolet photoelectron spectroscopy (UPS (HeI)), and temperature programmed desorption (TPD). To acquire detailed information regarding the initial stages of adsorption, TPD data, providing information about the relative surface coverage and the molecule-surface interaction, are compared directly with MIES data, which provide information about the electronic structure of the adsorbed molecules. For water adsorption, a prominent multilayer desorption feature develops in the TPD before the entire surface is covered, indicating 3D growth on the partially covered MgO(100)/Mo(100) surface. On the other hand, the formation of a methanol multilayer desorption feature coincides with complete coverage of the surface.

1. Introduction

For the detection of water and methanol on the MgO surface we have employed metastable impact electron spectroscopy (MIES), ultraviolet photoelectron spectroscopy (UPS), and thermal programmed desorption (TPD). MIES is an electron spectroscopic technique which provides a superior surface sensitivity and allows direct imaging of the local density of occupied states on the surface via the Auger deexcitation (AD) process (see ref 1 for a review). Due to its surface band gap of about 7 eV, MIES spectra taken from the MgO(100) surface are clearly dominated by the AD process.

The deexcitation of a metastable helium atom near a surface is a complex mechanism, governed by the overlap between the substrate and projectile orbitals. For that reason, very detailed information about the electronic structure of the outermost surface is necessary in order to reach quantitative conclusions regarding the MIES data. Such information is usually not available. However, in a recent MIES study[2] relative surface concentrations in a binary liquid mixture have been successfully determined. Furthermore, Kubiak et al.[3] showed that MIES spectra obtained from a partially oxidized Ni(100) surface could be modeled as a linear combination of spectra taken from clean Ni, oxygen-covered Ni, and a NiO surface. The results of references 2 and 3 serve as a basis for the discussion of our MIES data, supplemented by TPD, with respect to the growth mode, i.e., wetting versus clustering, of water and methanol on the MgO(100)/Mo(100) surface. Since MIES exclusively probes the electronic structure of the outermost substrate surface, one closed-packed monatomic or monomolecular adsorbate layer is sufficient to render the substrate essentially invisible. Besides monitoring a coverage dependent change in the surface electronic structure, this facilitates an estimation of the exposure at which the entire surface is covered, i.e., all substrate intensity vanishes.

Water and methanol on the MgO(100)/Mo(100) surface have been the subject of numerous studies. For example, the chemisorption of water has been addressed experimentally[4−10] and theoretically.[11−16] Frequently in these studies the absolute surface coverage is calibrated either by the saturation or the appearance of certain desorption features in TPD.[17,18] However, this coverage determination is accurate only if the adsorbate in question exhibits a well-ordered, layer-by-layer growth mode.

In the present study, MIES and TPD data have been obtained as a function of the coverage of methanol and water on MgO(100). A direct comparison of the MIES and TPD data reveals that multilayer water adsorption occurs before the entire surface is covered by water.

2. Experimental Section

The experiments were carried out in an ultrahigh vacuum (UHV) system (base pressure $<2 \times 10^{-10}$ Torr), which has been described in detail previously. Briefly, the UHV system consists of two interconnected chambers, one for sample treatment, low energy electron diffraction (LEED) and TPD, and the other for electron spectroscopy. The latter is equipped for X-ray photoelectron spectroscopy (XPS), Auger electron spectroscopy (AES), UPS, and MIES. TPD experiments were carried out using a differentially pumped quadrupole mass spectrometer (QMS). TPD spectra were collected at a linear heating rate of 3 K/s with the sample in line-of-sight to the QMS. MIES and UPS spectra were measured simultaneously using a cold-cathode discharge source[19,20] that provides both ultraviolet photons (HeI) and metastable He* $2^3S/2^1S$ ($E^* = 19.8/20.6$ eV) atoms with thermal kinetic energy. Metastable and photon contributions to the signal were separated by means of a time-of-flight method using a mechanical chopper. The collection of a MIES/UPS spectrum requires approximately 180 s. MIES and UPS spectra were acquired with an incident photon/metastable beam at 45° with respect to the surface normal in a constant pass energy mode using a double pass cylindrical mirror analyzer (CMA). The energy denoted by E_F in the spectra corresponds to electrons emitted from the Fermi level of the Mo(100) substrate. In the following spectra, all binding energies are referenced to E_F. Since the metallic Mo substrate and the analyzer are in electrical

* To whom correspondence should be addressed.

10.1021/jp992068a CCC: $19.00
Published on Web 05/25/2000

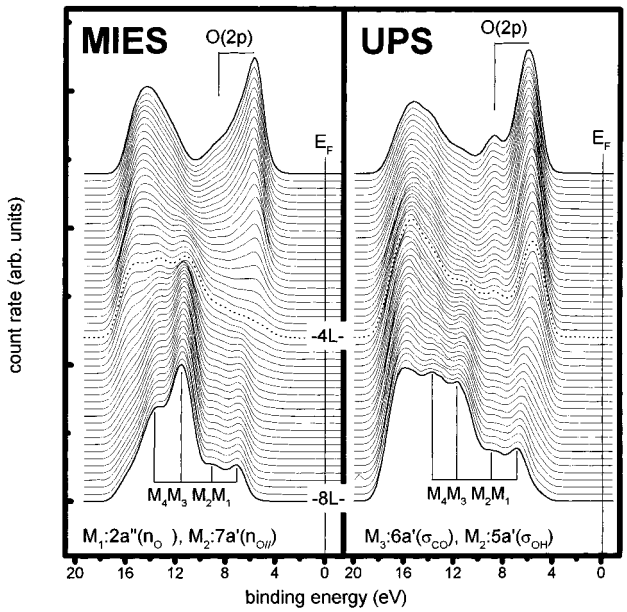

Figure 1. MIES and UPS spectra from a 100 K MgO(100)/Mo(100) substrate as a function of CH_3OH exposure. The uppermost spectrum shows the clean MgO(100) surface; the bottom spectrum shows the methanol-covered surface.

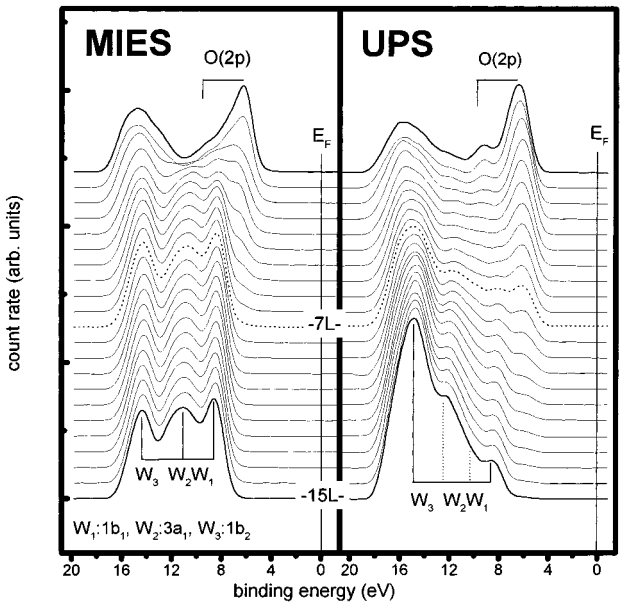

Figure 2. MIES and UPS spectra from a 100 K MgO(100)/Mo(100) substrate as a function of D_2O exposure. The uppermost spectrum shows the clean MgO(100) surface; the bottom spectrum shows the water-covered surface.

contact, the Fermi energy appears at a constant position (see ref 21 for more details).

MgO films (approximately 4 monolayers thick) were grown by depositing Mg in 1×10^{-6} Torr O_2 ambient on the Mo(100) surface at 550 K, followed by a 20 min annealing at 750 K in a 1×10^{-8} Torr O_2 background. The Mg source was made from a high-purity Mg ribbon wrapped around a tantalum filament. As shown in previous investigations, MgO films prepared under these conditions grow epitaxially on the Mo(100) substrate and their properties regarding the adsorption of water are comparable to those of MgO single crystal.[6,10,22] The quality of the MgO layers was checked with MIES, UPS, AES, and LEED. Water and methanol were dosed to the surface following the previously described procedure.[10,23] D_2O (CIL, 99.9%) and methanol (EM, 99.99%) were used after further purification via several freeze−pump−thaw cycles (vacuum distillation). Finally, both molecules were dosed to the sample from separate leak valves by backfilling the UHV system. Since the exposure in Langmuir ($1\ L = 1 \times 10^{-6}$ Torr s) for all dosed molecular species was determined with a nitrogen calibrated ion gauge, the given exposures are only useful as relative values. The stability of the respective partial pressures during dosage was monitored with a mass spectrometer. Relative coverages were determined by TPD and are correlated at each exposure with the MIES and UPS results.

3. Results

Electron Spectroscopic Results. Since the electron spectroscopic data acquired during exposure of water (D_2O) and methanol (CH_3OH) to the MgO-covered Mo(100) surface have been discussed in detail recently,[24,25] these data will only be briefly summarized here. Figure 1 presents a sequence of MIES and UPS spectra collected during methanol exposure to the MgO/Mo(100) surface. Methanol was dosed (0.18 L per spectrum) at a substrate temperature of 100 K. MIES and UPS spectra were recorded continuously during the exposure. The MIES and UPS spectra of the clean MgO(100) surface (uppermost spectra in Figures 1 and 2) agree well with those reported previously.[26] The structure denoted as O(2p) corresponds to emission from the O 2p valence band of the MgO(100) substrate. Due to the insulating character of the clean MgO(100) surface, no intensity between E_F and 3.8 eV binding energy is apparent. Thus no occupied states exist in resonance with the impinging He 2s electron, resulting in MIES spectra dominated by the Auger deexcitation (AD) process, which in turn allows a direct comparison between MIES and UPS data.[27] In both UPS and AD the kinetic energy E_{kin} of the emitted electrons follows the basic equation $E_{kin} = E_{exc} - E_{bin}$, where E_{exc} is the excitation energy of the projectile, i.e., 19.8 eV for metastable He(2^3S) atoms and 21.2 eV for UV(HeI) photons, and E_{bin} the binding energy of a substrate electron. For that reason, we can expect prominent features in the surface density of states (SDOS) to appear at the same binding energies in MIES and UPS. However, the selection rules for photoionization and AD are quite different. Due to the exchange-type interaction of the metastable helium atom with the surface, AD is particularly sensitive to those orbitals that protrude farthest into the vacuum, whereas UPS probes the average character of the several top layers.

TABLE 1: Binding Energies and Molecular Orbital Assignments for the Observed Methanol and Water Bands According to References 28, 30, 31, and 32

peak assignment	molecular orbital	binding energy
M_1	$2a''(n_{O\perp})$	7.1 eV
M_2	$7a'(n_{O//})$	9.2 eV
M_3	$6a'(\sigma_{CO})$	11.5 eV
M_4	$5a'(\sigma_{OH})$	13.4 eV
W_1	$1b_1$	7.7 eV
W_2	$3a_1$	9.9 eV
W_3	$1b_2$	13.3 eV

From the uppermost spectra in Figure 1, reflecting the SDOS of the clean MgO substrate, a continuous change in spectra which resembles those of gas phase[28] and condensed[29] methanol is observed. Binding energies and molecular orbital assignments for the four methanol induced features M_1, M_2, M_3, and M_4 based on gas-phase photoelectron and Penning ionization electron spectra (PIES)[28] are presented in Table 1. After an exposure of approximately 4 L (dotted spectra), the complete disappearance of the pronounced O(2p) structure in MIES

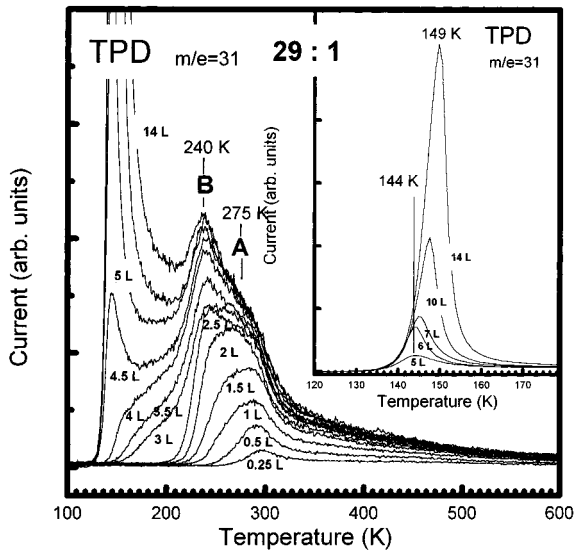

Figure 3. TPD spectra (3K/s) taken from the MgO(100)/Mo(100) surface as a function of the initial methanol (CH_3OH) coverage at 100 K. The inset presents the low-temperature desorption feature over an enlarged temperature scale.

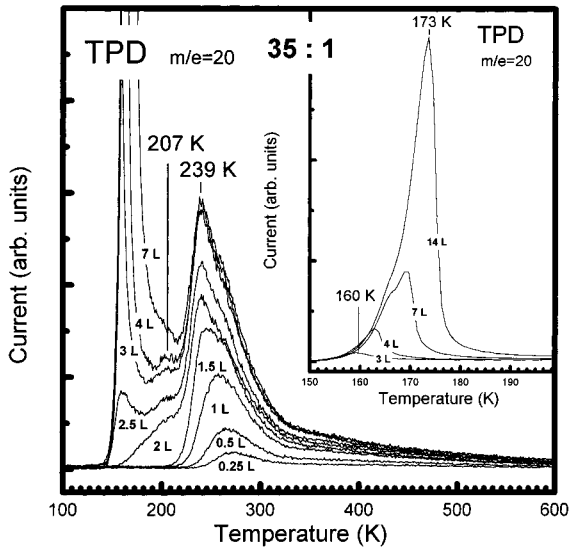

Figure 4. TPD spectra (3 K/s) taken from the MgO(100)/Mo(100) surface as a function of the initial water (D_2O) coverage at 100 K. The inset presents the low-temperature desorption feature over an enlarged temperature scale.

indicates that the entire surface is covered by methanol. Due to the limited surface sensitivity of UPS, the corresponding 4 L UPS spectrum shows an attenuated, but still distinct O(2p) band.

Figure 2 presents a sequence of MIES and UPS spectra collected during water (D_2O) exposure to the MgO covered Mo(100) surface. Water was dosed (0.7 L per spectrum) at a substrate temperature of 100 K. The uppermost spectra in Figure 2 show the clean MgO surface; the bottom spectra the surface covered by 15 L water. Binding energies and molecular orbital assignments for the three water induced structures W_1, W_2, and W_3 based on gas-phase photoelectron spectra[30,31] and PIES[32] are presented in Table 1. At an exposure of 7 L (dotted spectra) the MgO substrate intensity has virtually disappeared, indicating that the entire surface is covered by water. At this coverage UPS still shows a distinct O(2p) band, as expected for a thin water adlayer, but it is relatively less pronounced than the O(2p) feature in Figure 1 after the formation of a closed methanol layer at 4 L.

TPD Results. TPD spectra acquired from the MgO/Mo(100) surface precovered by various amounts of methanol and water at 100 K are presented in Figure 3 and Figure 4, respectively. In the temperature range from 100 to 600 K, basically two distinct desorption features are apparent in both figures, that is, a high-temperature peak at temperatures over 200 K, assigned to the desorption of chemisorbed molecules in direct contact with the substrate surface, and a low-temperature peak at temperatures below 190 K. The latter appears at higher exposures only and is assigned to the desorption of condensed molecular multilayer species. The inset in both figures presents the low-temperature desorption feature versus an enlarged temperature scale. In case of water on MgO thin layers and single crystals,[10,18] an additional desorption feature at 207 K appears at medium coverages. This peak, visible in Figure 4 between 2.5 and 4 L, corresponds either to the desorption of second layer water[18] or to first layer water with an uniquely different adsorption configuration.[10]

In accordance with previous studies, the low-temperature desorption feature of physisorbed water at exposures higher than 4 L (see inset in Figure 4) exhibits a shoulder at about 165 K. This shoulder is typically attributed to the irreversible phase transformation of amorphous solid water (ASW) to crystalline ice.[33] The corresponding desorption feature for methanol (see inset in Figure 3) does not show such a shoulder.

The high-temperature desorption feature corresponding to chemisorbed methanol (Figure 3) clearly exhibits an asymmetric structure, which can be separated into three parts: (i) at low exposures a peak arises denoted as A at 275 K, with (ii) a desorption tail that extends toward higher temperatures and (iii) a feature B at 240 K at exposures over 2 L. It is likely that B arises from the same phenomenon as A, that is, desorption of undissociated molecules in direct contact with the substrate. That these molecules are more easily desorbed is due to either an intermolecular repulsion in the more crowded overlayer or to the population of less favorable adsorption sites with increasing methanol coverage. The calculated desorption activation energies, according to the Redhead method[34] assuming first-order desorption kinetics and a preexponential factor of 10^{13} s^{-1}, are 73 and 62 kJ/mol for peaks A and B, respectively.

In Figure 4, the high-temperature desorption peak of chemisorbed water at ca. 250 K is asymmetric as well at coverages over 1.5 L; however, deconvolution into its component peaks is not possible. A slight but continuous shift of the peak maximum toward low desorption temperatures at increasing coverages could be interpreted as second-order desorption kinetics indicative of dissociative chemisorption. However, even on vacuum cleaved MgO(100) single-crystal surfaces, a slight shift toward lower binding energies is observed at low water coverages.[18] For the high-temperature desorption peak at saturation, an activation desorption energy of 61 kJ/mol is estimated.

The desorption tail at temperatures over 300 K in Figures 3 and 4 most likely originates from a more complex interaction between the MgO surface and the adsorbed molecular species.[35]

4. Discussion

The MIES and UPS data in Figures 1 and 2 illustrate the enhanced surface sensitivity of MIES. At 4 L methanol coverage in Figure 1, the complete disappearance of the substrate O(2p) intensity indicates that the entire MgO surface is covered by methanol. In contrast, UPS still shows a pronounced O(2p) peak at this coverage. At higher binding energies the adsorbate-induced bands M_3 and M_4 develop in MIES and UPS simultaneously. From these observations we deduce that methanol

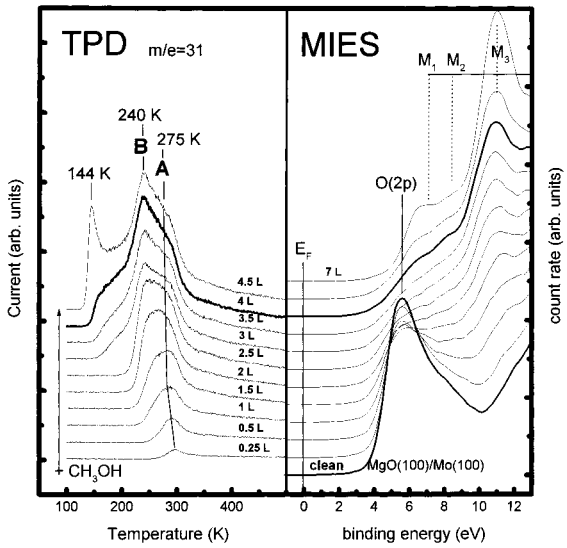

Figure 5. Comparison between TPD and MIES data taken from the MgO(100)/Mo(100) surface as a function of the methanol (CH_3OH) dosage at 100 K.

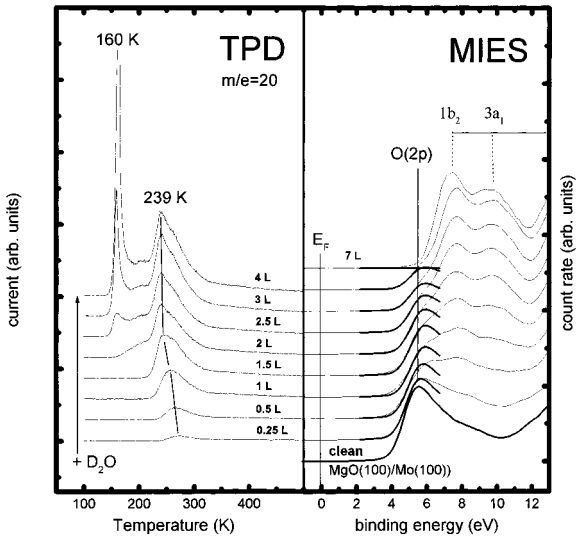

Figure 6. Comparison between TPD and MIES data taken from the MgO(100)/Mo(100) surface as a function of the water (D_2O) dosage at 100 K.

forms a uniform monomolecular layer on the MgO surface. This conclusion is supported by the fact that the condensation energy on the MgO surface (73 kJ/mol) is significantly higher than the sublimation energy of bulk methanol (35 kJ/mol), as calculated from the 6 L high- and low-temperature desorption maxima in Figure 3 (see also 36). Furthermore, we assume, according to previous studies,[25,37] that methanol adsorbs essentially nondissociatively with the OH groups oriented predominately toward the MgO surface. The appearance of two high-temperature desorption peaks A and B, as shown in Figure 3, suggests in this context a repulsive interaction between the methanol molecules in the first monolayer. Since B appears with a relatively high intensity, it is unlikely to arise from adsorption at defect sites, which, however, would likely provide a higher rather than lower adsorption energy. On the basis of an interactive model for species adsorbed on a 4-fold surface mesh,[38] assuming adsorption at thermodynamic equilibrium on specific and equivalent surface sites with the nearest neighbor interaction independent of coverage, an interaction energy between adjacent methanol molecules of approximately 2.8 kJ/mol is estimated. This relatively weak intermolecular repulsion, likely due to a van der Waals interaction of approximately parallel oriented molecules, is contradictory to strong lateral water−water attractions.[9] Interestingly, there are no apparent major differences in the desorption spectra between water and methanol in TPD, suggesting comparable adsorbate−substrate interactions for both species. However, as will shown in the following discussion, their ability to wet the surface appears to be quite different.

Figure 5 compares MIES with TPD spectra taken from a MgO/Mo(100) surface at various methanol coverages; subsequently, a MIES spectrum at the respective coverage of the TPD was carried out. The MIES spectra cover the same spectral range as in Figure 1; however, due to our interest in the structure close to the valence band maximum, only data in a binding energy range to 12 eV are shown. Furthermore, the energy scale in Figure 5 is reversed relative to Figures 1 and 2 to facilitate correlation between the data. It should be noted that for a respective methanol exposure, as indicated on the left panel, MIES and TPD spectra appear at the same *y*-offsets. On the right panel, the bottom MIES spectrum shows the clean MgO surface. Toward the uppermost spectrum, the methanol exposure increases as denoted in the figure. A comparison between MIES and TPD data reveals that the complete disappearance of the MgO substrate intensity in MIES at 4 L coincides with the appearance of a prominent low-temperature desorption feature, seen at 4.5 L. This observation supports the viewpoint, that methanol wets the MgO(100) surface effectively, that is, forms a closed-packed, two-dimensional structure before three-dimensional growth occurs. It is important to note that this interpretation is based on the assumption that the complete disappearance of the substrate intensity in MIES corresponds to the formation of a closed methanol adlayer. However, we are unable to give an exact definition of how dense this layer has to be in order to shield the substrate for MIES completely. On the other hand, it appears quite reasonable to assume that residual substrate intensity in MIES is indicative of an incompletely covered surface, which will be a strong argument in the following discussion of the data obtained from a water-covered MgO surface.

Figure 6 compares, in the same fashion as Figure 5, MIES and TPD data obtained at various water exposures to the MgO(100) surface. On the right panel, the bottom MIES spectrum shows the clean MgO substrate; the uppermost, the surface completely covered by water (7 L). Between, spectra of the partially water-covered MgO surface have been fitted by a linear combination of the bottom and the uppermost spectrum in order to determine the amount of MgO substrate intensity contributing to the respective spectrum. During the fitting procedure, the intensities of the bottom and the uppermost spectrum have been varied. For acquiring work function changes during the water adsorption, the positions of both spectra have been varied until an excellent agreement between fit and measurement has been reached. The MgO substrate intensities obtained in this way are presented in bold between 2 and 7 eV in the figure. The assumption that clean and water-covered areas coexist simultaneously on the MgO surface and appear in MIES with an intensity only proportional to their lateral extension on the surface, would then allow an estimation of the surface area covered by water. However, this model appears quite simple since it links the electronic structure of an adsorbate and its appearance in MIES to a lateral surface coverage without considering the complex interaction between the adsorbed species and the impinging metastable helium atom. For that reason we will not discuss in detail the attenuation of the MgO

substrate intensity as a function of the water coverage; however, we will use its appearance as an indicator for the incomplete covered surface.

In Figure 6 at 2.5 L, the appearance of the low-temperature desorption state indicates that at this exposure a significant amount of water condenses in a second layer configuration. However, a persistent, substantial MgO substrate intensity argues against the suggestion that this adsorption occurs after formation of a closed-packed layer of water molecules in direct contact with the substrate. Even after formation of a prominent multilayer desorption feature at 4 L, the MgO surface appears incompletely covered. This could be exclusively a feature of the MgO layers prepared in the present study, e.g., the preparation of the MgO layers may result in high index planes[39] which may be incompletely covered by water. However, methanol wets the same substrate effectively. Different intermolecular interactions between methanol and water are more likely a reason for the observed efficiencies in wetting the MgO surface.

In refs 9 and 10 it is shown that an ordered water adlayer with $c(4 \times 2)$ symmetry is formed on MgO(100) below 185 K at saturation coverage with a water partial pressures $<10^{-9}$ mbar. Heating the substrate above 185 K results in partial desorption of water and the formation of a less dense water adlayer with $p(3 \times 2)$ symmetry. A correlation of the intermediate desorption state at 207 K in Figure 4 with such a phase transition is a possibility. Taking the strong intermolecular water attraction into consideration, it is plausible that at submonolayer coverages 2D island formation is favored. From a kinetic point of view, mobile precursor mediated adsorption as suggested in ref 18 supports this model. With this assumption, it is expected that, at a certain island size (due to a limited molecular diffusion length), second layer condensation will occur. This island size is then determined by the maximum diffusion length of the water molecules in an adsorption precursor before being trapped into a second layer by H-bonding.[40] That the strong intermolecular attraction in submonolayer water is mainly electrostatic[40] could explain the dramatic difference between the water−water and methanol−methanol interaction energies simply via a steric model. For water on MgO(100) it is assumed that the molecules are lying with their planes approximately parallel to the surface, while the methanol molecules adsorb in a configuration with the C−O bond essentially parallel to the surface and the OH groups oriented toward the surface. For a parallel orientation and for polarized methanol molecules the observed weak repulsive interaction appears plausible. Methanol molecules may bind to the MgO surface with a strength comparable to water, but the small intermolecular repulsion results at low coverages in the formation of a loosely packed adlayer, which has the tendency to wet the surface. The suggestion of a comparable adsorbate−substrate interaction energy for water and methanol is in accordance with the TPD data, but appears inconsistent with the isosteric heat of condensation of approximately 85 kJ/mol for water in the $p(3 \times 2)$ phase. However, this energy is partially due to a reversible 2D gas−solid transition[9] where dissolution of the 2D solid prior to desorption would result in an activation desorption energy governed by the adsorbate−substrate interaction.

Unfortunately, in the present investigation, we are unable to compare data obtained from thin MgO layers grown on Mo(100) and a MgO(100) surface obtained by vacuum cleavage. For that reason, we cannot completely exclude the possibility that our data are characteristic of MgO thin layers only.

5. Summary

The present study compares MIES data, providing information of the surface electronic structure, and TPD data, providing information of the relative surface coverage and the molecule−surface interaction, taken from the MgO/Mo(100) surface at various methanol and water coverages. For the water adsorption, it is found that a prominent multilayer desorption feature develops in TPD before the entire surface is covered. This result indicates second layer condensation on the partially water covered MgO(100)/Mo(100) surface. In case of methanol adsorption, the relative rapid disappearance of the MgO substrate intensity in an exposure regime where TPD shows only a high-temperature desorption feature (up to 2.5 L) indicates more effective wetting of the MgO(100)/Mo(100) surface by methanol.

Acknowledgment. We acknowledge with pleasure the support of this work by the National Science Foundation and the Robert A. Welch Foundation.

References and Notes

(1) Harada, Y.; Masuda, S.; Ozaki, H. *Chem. Rev.* **1997**, *97*, 1897.
(2) Morgner, H.; Oberbrodhage, J. *J. Electron. Spectrosc. Relat. Phenom.* **1997**, *87*, 9.
(3) Kubiak, R.; Morgner, H.; Rakhovskaya, O. *Surf. Sci.* **1994**, *321*, 229.
(4) Peng, X. D.; Barteau, M. A. *Surf. Sci.* **1990**, *233*, 283.
(5) Karolewski, M. A.; Cavell, R. G. *Surf. Sci.* **1992**, *271*, 128.
(6) Wu, M.-C.; Estrada, C. A.; Corneille, J. S.; Goodman, D. W. *J. Chem. Phys.* **1992**, *95*, 3892.
(7) Heidberg, J.; Redlich, B.; Wetter, D. *Ber. Bunsen.-Ges Phys. Chem.* **1995**, *99*, 1333.
(8) Ferry, D.; Glebov, A.; Senz, V.; Suzanne, J.; Toennies, J. P.; Weiss, H. *J. Chem. Phys.* **1996**, *105*, 1697.
(9) Ferry, D.; Glebov, A.; Senz, V.; Suzanne, J.; Toennies, J. P.; Weiss, H. *Surf. Sci.* **1997**, *377*, 634.
(10) Xu, C.; Goodman, D. W. *Chem. Phys. Lett.* **1997**, *265*, 341.
(11) Scamehorn, C. A.; Hess, A. C.; McCarthy, M. I. *J. Chem. Phys.* **1993**, *99*, 2786.
(12) Langel, W.; Parrinello, M. *J. Chem. Phys.* **1995**, *103*, 3240.
(13) Chacon-Taylor, M. R.; McCarthy, M. I. *J. Phys. Chem.* **1996**, *100*, 7610.
(14) de Leeuw, N. H.; Watson, G. W.; Parker, S. C. *J. Chem. Soc., Faraday Trans.* **1996**, *92*, 2082.
(15) Tikhomirov, V. A.; Geudtner, G.; Jug, K. *J. Phys. Chem. B 101*, 10398.
(16) Soetens, J. C.; Millot, C.; Hoang, P. N. M.; Girardet, C. *Surf. Sci.* **1998**, *419*, 48.
(17) Zhou, X.-L.; Cowin, J. P. *J. Phys. Chem.* **1996**, *100*, 1055.
(18) Stirniman, M. J.; Huang, C.; Smith, R. S.; Joyce, S. A.; Kay, B. D. *J. Chem. Phys.* **1996**, *105*, 1295.
(19) Maus-Friedrichs, W.; Wehrhahn, M.; Dieckhoff, S.; Kempter, V. *Surf. Sci.* **1990**, *237*, 257.
(20) Maus-Friedrichs, W.; Dieckhoff, S.; Kempter, V. *Surf. Sci.* **1991**, *249*, 149.
(21) Kantorovich, L. N.; Shluger, A. L.; Sushko, P. V.; Günster, J.; Stracke, P.; Goodman, D. W.; Kempter, V. *Faraday Discuss.* **1999**, *114*, 173.
(22) Wu, M.-C.; Truong, C. M.; Goodman, D. W. *Phys. Rev. B* **1992**, *46*, 12688.
(23) Parmeter, J. E.; Jiang, X.; Goodman, D. W. *Surf. Sci.* **1990**, *240*, 85.
(24) Günster, J.; Liu, G.; Kempter, V.; Goodman, D. W. *J. Vac. Sci. Technol. A* **1998**, *16*, 996.
(25) Günster, J.; Liu, G.; Stultz, J.; Goodman, D. W. *J. Chem. Phys.* **1999**, *110*, 2558.
(26) Ochs, D.; Maus-Friedrichs, W.; Brause, M.; Günster, J.; Kempter, V.; Puchin, V.; Shluger, A.; Kantorovich, L. *Surf. Sci.* **1996**, *365*, 557.
(27) Ertl, G. *Surf. Sci.* **1997**, *89*, 525.
(28) Yamakado, H.; Yamauchi, M.; Hoshino, S.; Ohno, K. *J. Phys. Chem.* **1995**, *99*, 17093.
(29) Paul, J. *Surf. Sci.* **1985**, *160*, 599.

(30) Turner, D. W.; Baker, C.; Baker, A. D.; Brundle, C. R. *Molecular Photoelectron Spectroscopy*; Wiley: New York, 1970.

(31) Banna, M. S.; McQuaide, B. H.; Malutzki, R.; Schmidt, V. J. *Chem. Phys.* **1986**, *84*, 4739.

(32) Cermak, V.; Yencha, A. J. *J. Electron Spectrosc. Relat. Phenom.* **1977**, *11*, 67.

(33) Smith, R. S.; Huang, C.; Kay, B. D. J. *Phys. Chem. B* **1997**, *101*, 6123.

(34) Redhead, P. A. *Vacuum* **1962**, *12*, 203.

(35) Giordano, L.; Goniakowski, J.; Suzanne, J. *Phys. Rev. Lett.* **1998**, *81*, 1271.

(36) *Zahlenwerte und Funktionen aus Naturwissenschaften und Technik*, Neue Serie; Landolt-Börnstein, 5th ed.; Springer: Berlin, 1923; p 1482.

(37) Street, S. C.; Xu, C.; Goodman, D. W. *Annu. Rev. Phys. Chem.* **1997**, *48*, 43.

(38) King, D. A. *Surf. Sci.* **1975**, *47*, 384.

(39) Gallagher, M. C.; Fyfield, M. S.; Cowin, J. P.; Joyce, S. A. *Surf. Sci.* **1995**, *339*, L909.

(40) Girardet, C.; Hoang, P. N. M.; Marmier, A.; Picaud, S. *Phys. Rev. B* **1998**, *57*, 11931.